THE UNIVERSITY of EDINBURGH

Edinburgh Research Explorer

Analysis of CO2 kinetics in Na,Cs-Rho crystals using the Zero Length Column – a case study for slow systems

OPEN ACCESS

Analysis of CO$_2$ kinetics in Na,Cs-Rho crystals using the zero length column: a case study for slow systems

Enzo Mangano[1] · Stefano Brandani[1]

Abstract

Experimental measurements of systems with slow gas transport kinetics are generally considered a relatively easier task when compared to the challenges of measurements of very fast systems. On the other hand, when the transport process goes towards time constants of the order of several hours, not only the measurements, but also the analysis and interpretation of the data offer challenges which make the assessment of the correct time constant of the process non trivial. In this work we used the measurements of CO$_2$ diffusion in Na,Cs-Rho crystals, carried out using the zero length column (ZLC) technique, as a case study for the use of the technique for very slow adsorption processes. The system, which has a time constant of the order of 8 h, shows the importance of using the partial loading approach for the determination of an unambiguous time constant from the analysis of the ZLC desorption curves. The traditional analysis is refined by using the nonlinear ZLC model to take into account the isotherm nonlinearity that results in a concentration dependent diffusivity. Finally, the method proposed by Cavalcante is used to confirm the 3-D diffusion path of the system.

Keywords Adsorption · ZLC technique · Slow diffusing systems · Carbon dioxide · Rho zeolite

Abbreviations

a_n	Pre-exponential factor in the analytical solution of fluid phase concentration
b	Langmuir parameter, m^3/mol
c	Concentration in the fluid phase, mol/m^3
$\bar{c}$	Average concentration in the fluid phase, mol/m^3
c_0	Initial concentration in the fluid phase, mol/m^3
c_S	Fluid phase concentration at the second switch of the partial loading experiment, mol/m^3
D	Diffusion coefficient, m^2/s
D_0	Diffusivity at infinite dilution, m^2/s
F	Volumetric flowrate, m^3/s
K	Dimensionless Henry law constant
l	Half-thickness of slab geometry, m
L	Dimensionless parameter in ZLC model defined in Eq. 4
L_{app}	Dimensionless parameter in ZLC model for the slab geometry, Eq. 7
L_s	Dimensionless parameter in ZLC model for the slab geometry, Eq. 7

$\bar{q}$	Average concentration in the adsorbed phase, mol/m^3
q_0	Initial concentration in the adsorbed phase, mol/m^3
q_s	Adsorbed phase concentration at saturation, mol/m^3
P	Pressure, Pa
R	Particle radius, m
t	Time, s
t_S	Time between the two switches in the partial loading experiment, s
V_S	Volume of solid, m^3
V_F	Volume of fluid, m^3

Greek letters

β_n	Eigenvalues of the diffusion equation
γ	Dimensionless parameter defined in Eq. 4
λ	Nonlinear parameter defined in Eq. 9
τ	Time constant $= \frac{R^2}{D}$, s

✉ Stefano Brandani
s.brandani@ed.ac.uk

[1] School of Engineering, University of Edinburgh, Edinburgh EH9 3FB, UK

Introduction

The zero length column (ZLC) technique was introduced in 1988 as an alternative method to measure accurately fast intra-crystalline diffusion in systems characterised by strong adsorption (Eic and Ruthven 1988). The main experimental challenges when dealing with fast systems lie not only in

designing a system that can reliably detect quick changes in the monitored concentration (i.e. a system designed with a faster intrinsic kinetics then the mass transport) but, more importantly, in minimising heat effects generated due to the rapid adsorption process. The design of the ZLC, based on the use of a very small amount of sample in a monolayer setup with a relatively large flow of gas per mass of sample, has the key advantage of minimising both bed resistance and heat effects, allowing the determination of the mass transport kinetics with no intrusion of secondary resistances. During the past three decades, the ZLC has seen a number of improvements and adaptations, which have broadened the application of the technique to a wide variety of systems. In a recent review, we have described how the technique has evolved over the years to allow measurements of different kinetic regimes as well as equilibrium processes, highlighting good practices and pitfalls in the use of the methodology (Brandani and Mangano 2021). Clearly, moving to slower adsorption processes helps to mitigate the effects of secondary resistances therefore it simplifies the experimental approach to the measurements. On the other hand, the interpretation of the results when processes have time constants of the order of several hours, reveals some challenges.

The first ZLC measurements on slow systems were carried out by Cavalcante and Ruthven (1995) who were looking at the kinetics of C6 paraffins in silicalite. These systems are particularly interesting because the dimensions of the molecules are very close to the size of the silicalite channels, resulting in a very slow diffusion process due to the steric resistance. Most of the uptake rate experiments were carried out using a gravimetric system, but as explained by the authors, even if all possible precautions were taken to ensure isothermality (small mass, small pressure incremental steps) the ZLC was used to confirm some of the results. Undesired effects such heat resistance or crystal size distribution can in fact be easily mistaken for slow diffusion processes therefore the ZLC proved to be a useful tool to show that the large time constants (up to about 7 h) were indeed a hindered diffusion process.

The same authors expanded the study by using the ZLC to investigate the diffusion of a series of paraffins (nC6–nC20) in offretite-erionite intergrowth crystals (Cavalcante et al. 1995). The study was of particular relevance as it showed the expected monotonic decrease of the diffusivity with the carbon number, being one of the first studies to disprove the so-called "window effect" theory (Cavalcante et al. 1995; Magalhães et al. 1996) used to explain an unusual trend of diffusivities of paraffins in zeolite T (Gorring 1973). With time constants as large as almost 20 h, to the best of our knowledge, Cavalcante et al. (1995) report the slowest systems ever measured with a ZLC system. In order to confirm the time constant measured with the classical ZLC long time approach the authors introduced the intermediate time analysis. This has the added advantage of allowing an easy check of the diffusion path, i.e. to discern between 3-D isotropic and one-dimensional diffusion. By using this combined approach, the authors not only confirmed the time constants obtained but also clearly identified the slab diffusion mechanism for the pure offretite sample which was also in line with the geometry of the sample (Cavalcante et al. 1995, 1997).

Hindered diffusion is generally associated with the case in which the size of the probe molecule is very close to the size of the channels of the adsorbent. This is a relatively well established and understood phenomenon. In more recent years, the development of new materials with complex structures has given rise to a number of unconventional transport behaviours. Among these, adsorbents with flexible structures which undergo structural transition, typically MOFs (Remy et al. 2011; Zhao et al. 2016; Serre et al. 2002) or zeolites(Palomino et al. 2012; Lozinska et al. 2014; Greenaway et al. 2015; Li et al. 2017), are probably the ones that have received more interest. What makes these materials of interest is that their structural changes are mostly triggered by a specific adsorbate concentration and can manifest, for example, as a change of the cage volume, breathing (Barthelet et al. 2002) or gate opening (Georgieva et al. 2019; Lozinska et al. 2012), therefore opening the possibility to finely control their kinetic and/or equilibrium selectivity during the adsorption process. Among zeolites, the Rho-types are probably the most renowned for this feature. Their structure is characterised by a body-centred-cubic arrangement of α-cages connected by double eight-rings, with an effective channel diameter of about 3.6 Å (Baerlocher et al. 2007). These zeolites are characterised by a severe hindering effect caused mainly by the deformations to the structure induced by the extra-framework cations (Lee et al. 2001). Distribution and positioning of the cations inside the Rho structure have a key role in this steric effect to gas transport and may result in the so-called "molecular trapdoor" mechanism, in which only molecules having affinity with the cations (CO_2, for example) can "open" the trapdoor and access the cage, while other molecules are completely excluded (Lozinska et al. 2014; Shang et al. 2012, 2013). In a previous study (Lozinska et al. 2012), we have proved the use of the ZLC technique as a powerful tool to understand the CO_2 adsorption and transport mechanism in Na- and Na,Cs-Rho identifying, for the fully exchanged Na-Rho, a clear structural transition occurring during the desorption of CO_2. The Na,Cs-Rho sample did not show any evidence of structural modification, but its severe hindering effect resulted in a very slow CO_2 uptake rate with a time constant of about 8 h. In this contribution, we will use CO_2 in Na,Cs-Rho as an interesting case study to show the use of the ZLC analysis to extract the correct diffusional time constant of the process and, using the nonlinear model, the CO_2 isotherm parameters.

The ZLC technique

The model of the ZLC is based on the mass balance of an adsorption column in the limit of an infinitesimally short column, which effectively results into a perfectly mixed cell (Eic and Ruthven 1988). Assuming a single adsorbate in an inert carrier gas, the mass balance of the column is given by

$$V_S \frac{d\overline{q}}{dt} + V_F \frac{d\overline{c}}{dt} = (Fc)_{IN} - (Fc)_{OUT}, \tag{1}$$

where $\overline{c}$ is the average fluid phase concentration; $\overline{q}$ is the average adsorbed phase concentration; c is the fluid phase concentration; F is the volumetric flowrate at the temperature and pressure of the column; V_S is the volume of the solid in the column; and V_F is the volume of the fluid in the column. Under the assumption of equilibrium linearity and Fickian diffusion in a spherical particle, the solution of the dynamic response to a step change in concentration at the inlet from the initial concentration desorption c_0 to 0 can be derived as (Brandani and Mangano 2021; Brandani and Ruthven 1995)

$$\frac{c}{c_0} = \sum_n \frac{2L \exp\left(-\beta_n^2 \frac{D}{R^2} t\right)}{\beta_n^2 + \left(\gamma \beta_n^2 + 1 - L\right)^2 + \gamma \beta_n^2 + L - 1} = \sum_n a_n \exp\left(-\beta_n^2 \frac{D}{R^2} t\right), \tag{2}$$

where β_n is given by the root of

$$\beta_n \cot \beta_n + L - 1 - \gamma \beta_n^2 = 0. \tag{3}$$

The solution in Eq. 2 is determined by the dimensionless parameters

$$\gamma = \frac{1}{3} \frac{V_F}{KV_S} \quad L = \frac{1}{3} \frac{F}{KV_S} \frac{R^2}{D}, \tag{4}$$

where K is the dimensionless Henry law constant and $\frac{D}{R^2}$ the diffusional time constant. The dimensionless parameter γ represents the ratio of the accumulation in the fluid phase relative to that of the adsorbed phase; while L is the ratio between the diffusion time constant and the time constant of the washout of the adsorbed phase, $\frac{KV_S}{F}$. For strongly adsorbed components K is very large and therefore $\gamma \approx 0$. This simplifies Eq. 2 to the orginal solution derived by Eic and Ruthven (1988).

L is the key parameter that controls which regime the system is under. For $L \gg 1$, the system is transport limited, therefore under kinetic control. If $L < 1$, the system is under equilibrium control, i.e. the diffusion is so fast that the internal concentration profile inside the adsorbent is essentially flat. From the definition of L it is clear that by tuning the experimental conditions (flowrate, temperature and sample mass) it is possible to push the system towards equilibrium or kinetic regime, i.e. small samples and high flowrates are recommended for kinetic tests and the opposite for equilibrium controlled tests (Brandani and Mangano 2021).

An essential tool for kinetic experiments and especially for slow systems is the so-called partial loading experiment, where the experiments are run by preventing the sample to reach full equilibration in the adsortion step. In practice, the desorption starts after an adsorption step significantly shorter than the equilibration time, with the result of essentially imposing a time constant to the system (Brandani and Ruthven 1996; Brandani et al. 1995). The solution to the linear model for the case in which the system is partially loaded for a time t_s is given by

$$\frac{c}{c_S} = \frac{\sum_n a_n \left[1 - \exp\left(-\beta_n^2 \frac{D}{R^2} t_S\right)\right] \exp\left[-\beta_n^2 \frac{D}{R^2} \left(t - t_S\right)\right]}{1 - \sum_n a_n \exp\left(-\beta_n^2 \frac{D}{R^2} t_S\right)} \quad \text{for} \quad t \geq t_S, \tag{5}$$

where c_S is gas phase concentration at the switch of the partial loading experiment. From Eq. 5 it is clear that, being t_S imposed by the user, no additional parameters are required, therefore the partial loading experiment can be predicted from the parameters extracted from the full loading experiment. Matching both the partial and full loading curves ensures unambiguously that the correct time constant has been determined.

In some cases, it may be useful to couple the conventional long-time analysis with the intermediate time one (Hufton and Ruthven 1993). This approach, by looking at the early stages of desorption, is less affected by any baselining error, but at the same time it is more sensitive to any uncertainty in the time-zero of the desorption curve and therefore less reliable for very fast systems (Brandani and Ruthven 1996). The methodology has also the advantage to provide an easy way to discriminate between the spherical and slab diffusion model (Cavalcante and Ruthven 1995; Cavalcante et al. 1995). Solving the ZLC model for intermediate times the following expressions are obtained (Cavalcante et al. 1997; Hufton and Ruthven 1993)

$$\frac{c}{c_0} = \frac{1}{L} \left(\sqrt{\frac{R^2}{\pi D t}} - 1\right) \quad \text{sphere} \tag{6}$$

$$\frac{c}{c_0} = \frac{1}{L_s} \sqrt{\frac{l^2}{\pi D t}} \quad \text{slab} \tag{7}$$

To use properly the intermediate time analysis, Eqs. 6 and 7 should be used in the time range corresponding to $\frac{c}{c_0} < 0.2$ and for $L > 10$. In addition, all factors affecting the initial part of the desorption curve should be minimised, meaning that the method should be applied to relatively slow system, under linear conditions and with narrow particle size distribution (Brandani and Mangano 2021). In a plot $\frac{c}{c_0}$ vs $\sqrt{\frac{1}{t}}$, Eqs. 6 and 7 are straight lines with intercept at $-\frac{1}{L}$ or 0, therefore providing a clear distintion between the two diffusion paths (Cavalcante et al. 1997). A convenient way to display ZLC response curves at different flowrates is to plot $\frac{c}{c_0}L$ vs $\sqrt{\frac{1}{t}}$. In this plot, in fact, the solutions for different flowrates should reduce to the same straight line with intercept at -1 for Eq. 6 and 0 for Eq. 7.

Experimental

The ZLC apparatus used in this study is described in detail in previous publications (Hu et al. 2015a, b). The system is equipped with two sets of Brooks mass flow controllers that allow to operate the system under low and high flow conditions for equilibrium and kinetic experiments. Briefly, the experiment consists in flowing a mixture of 10% CO_2 in He (carrier gas) through the ZLC at a constant flowrate, once equilibration is achieved the inlet flow to the column is switched to the carrier and the desorption starts. The experimental procedure for the partial loading is exactly the same, but this time the adsorption step is considerably shorter to prevent the system to reach equilibrium. The outlet concentration of the ZLC is monitored using an Ametek Dycor Dymaxion quadrupole mass spectrometer and the raw signal is then converted to dimensionless concentration.

The Na,Cs-Rho crystals used were synthesised by Prof. Wright's group at the University of St. Andrews. A detailed characterisation is provided in a previous contribution (Lozinska et al. 2012). Images of the crystals acquired using a Jeol JSM-6700F high resolution Scanning Electron Microscope show 1 μm agglomerates of crystals of about 100 nm in diameter, Fig. 1. A 1/8″ Swagelok union with 11.6 mg of sample was packed for the ZLC experiments. Prior to the experiments the adsorbent was regenerated at 350 °C overnight under He flow. The regeneration procedure was carried out using a slow temperature ramp of 1 °C/min to 110 °C first, holding the temperature for 1 h and followed by a second ramp to 350 °C

Full loading experiments were carried out at 35 °C at flowrates ranging from 2 to 30 ml/min with additional partial loading runs at 2.1 and 8.4 ml/min to confirm the kinetic regime and assess reliably the time constant.

Experimentally, the first evidence of a slow adsorption process was the high dependency of the amount adsorbed
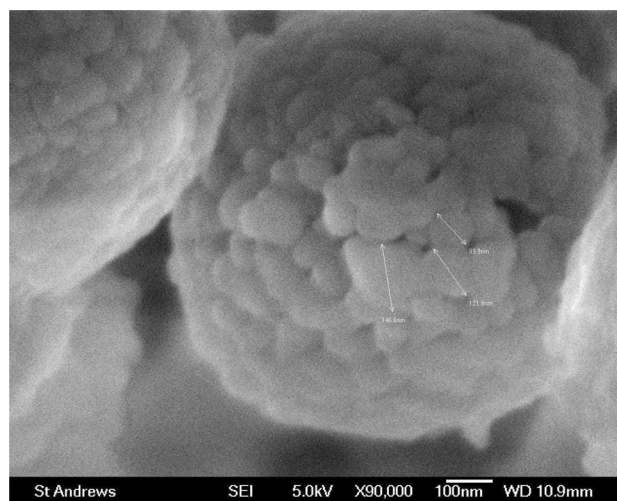

Fig. 1 SEM images of Na,Cs-Rho crystals

on the adsorption time. The monitored variable is in fact the concentration in the gas phase, and, in this case, the uptake is so slow that the outlet gas phase concentration is practically constant, resulting into a misleading stable plateau of the monitored signal. For this reason, running a quick partial loading test can provide a good indication of the time constant of the process and therefore fully equilibrate the sample by running an adsorption step for a time exceeding 0.5 R^2/D (Brandani and Ruthven 1996). The sample required about 8 h to achieve full equilibration.

Applying a mass balance to the column the amount of CO_2 adsorbed at equilibrium can be calculated. At 35 °C and 0.1 bar the CO_2 uptake on Na,Cs-Rho resulted in 2.13 mol/kg.

Results and discussion

As mentioned above the sample showed a considerably long equilibration time which is already an indication per se of the presence of a transport resistance. Nevertheless, to confirm the controlling regime a simple graphical check is available by plotting the ZLC desorption curves as c/c_0 vs Ft (Brandani 2016). Under equilibrium control the ZLC curves will overlap in an Ft plot, while if the curves cross the system is under kinetic control. Figure 2 shows the ZLC desorption curves for CO_2 in Na,Cs-Rho at two different flowrates both as t and Ft plots. The Ft plot shows the curves at different flowrates clearly intersecting, confirming the presence of a kinetic resistance.

Given the extremely slow kinetics, macropore resistances due to the crystal agglomerates shown in Fig. 1 can also be excluded. The CO_2 uptake and Henry law constant are similar to those of 13X zeolites, which should yield, in the

Fig. 2 ZLC desorption curves for Na,Cs-Rho at 2.1 ad 8.4 ml/min: **a** *t* plot; **b** *Ft* plot
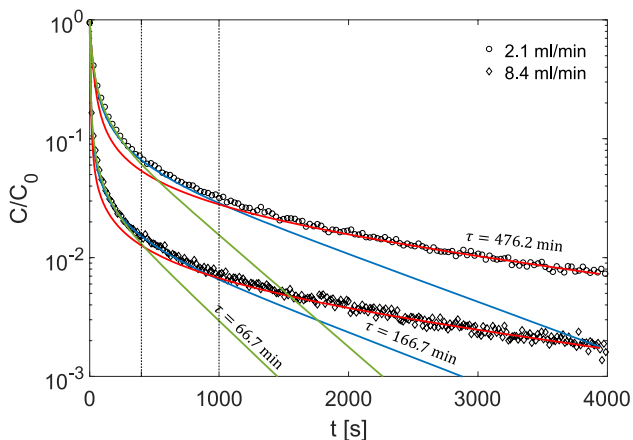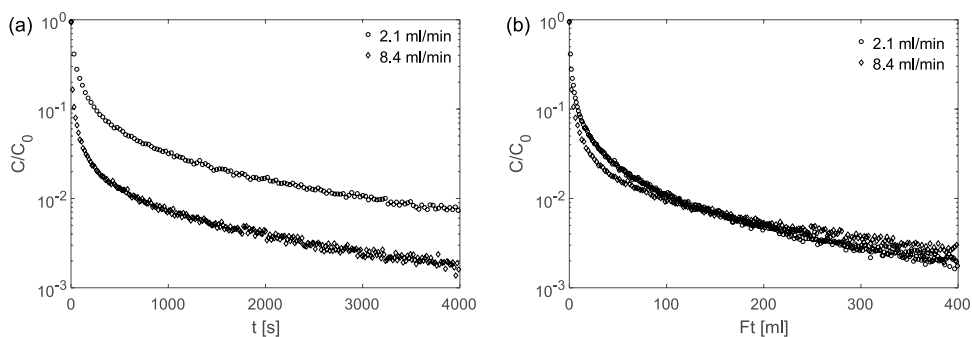

Fig. 3 ZLC desorption curves at 35 °C for CO_2 on Na,Cs-Rho analysed at three different observation times, 400, 1000 and 4000 s. Time constants ($\tau = \frac{R^2}{D}$) for each case are reported in the plot, vertical lines indicate the 400 and 1000 s markers

by a slowly varying exponential decay that extends for several hours. The main issue with such a behaviour is that it is not immediately obvious where the long-time asymptote should be taken to extract the kinetic constant. This is even more clear in the example shown in Fig. 3. Here the experimental curves are matched with the model predictions with different time constants extracted using the long-time asymptote corresponding to different range of times for the desorption (400, 1000 and 4000 s from the start of the desorption). For each time constant, τ, (or long-time asymptote), the standard ZLC model provides a very good match of both flowrates indicating that in this case relying only on the analysis of the full loading experiments does not allow to determine a time constant independent from the observation time (Brandani and Mangano 2021).

It is clear then that the use of the traditional full loading approach is not sufficient to solve this issue, while adding the partial loading runs can resolve the ambiguity.

Figure 4 shows the full and partial loading curves for 2.1 and 8.4 ml/min with the ZLC diffusion model predictions. Comparing this to Fig. 3 it is evident that only the time constant corresponding to the longest observation time allowed to match both flowrates and the corresponding partial loading experiment. Figure 4 includes also the predictions using
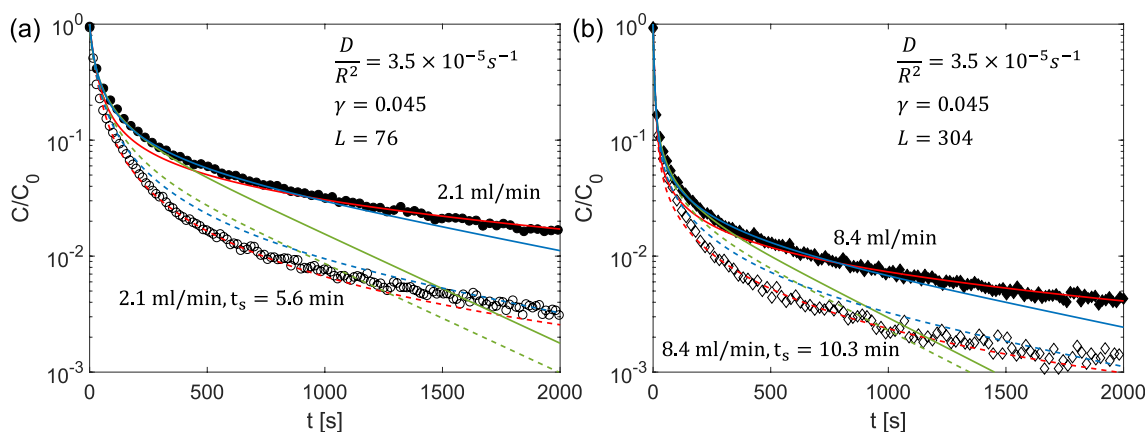
case of a macropore diffusion controlled regime, to a much quicker response in the order of seconds or minutes, not hours.

The *t* plot shows the expected profile of the ZLC experiment, but, due to the slow kinetics, the signal is characterised

Fig. 4 Full and partial loading ZLC curves of 10% CO_2 in Na,Cs-Rho at **a** 2.1 ml/min and **b** 8.4 ml/min with ZLC model predictions. Red: model parameters reported in the plot; Blue and Green: model predictions using time constants reported in Fig. 3

the time constants at shorter observation times used in Fig. 3. These clearly lead to the prediction of a faster process, resulting in a mismatch of the partial loading response, closer to the full loading compared to the experimental data (Brandani and Mangano 2021). The match of full and partial loading at two different flowrates confirms the correctness of the diffusivity obtained. Note also that the model parameters used are extracted from a curve at a single flowrate, knowing the partial loading time, t_s, the only flowrate-dependent parameter is L.

A closer inspection of the curves shows also a non-linearity effect evident in the small mismatch between the data and the model in the initial curvature of the full loading curves. This is also confirmed by the CO_2 isotherm measured at 25 °C and reported in our previous contribution (Lozinska et al. 2012). It should also be noted that the nonlinearity effect is not reflected in the partial loading response. In fact, due to the short adsorption time and the slow diffusion, the average adsorbed concentration inside the crystal is low enough to be essentially under linear equilibrium conditions (Brandani and Mangano 2021).

The solution for the ZLC model in presence of nonlinear equilibrium but constant diffusivity was derived by Brandani (1998). Compared to the linear ZLC model, there is one additional parameter if the Langmuir isotherm is used, Eq. 8.

$$\frac{q}{q_s} = \frac{bc}{1 + bc} \tag{8}$$

The resulting dimensionless nonlinearity parameter, λ, is given by

$$\lambda = \frac{q_0}{q_s} = \frac{bc_0}{1 + bc_0} \tag{9}$$

The key effect of nonlinearity is a shift of the long-time asymptote inducing a large uncertainty in the apparent L parameter, with $L_{app} = L_0/(1 - \lambda)$. The apparent L parameter is obtained applying the linear model to nonlinear experiments, which in this case are the values shown in Fig. 4.

As λ is reduced the system becomes linear. To obtain an improved match with the experimental results here the concentration dependence of the diffusivity according to the Darken correction is used. This is also only a function of λ and the initial concentration in the adsorbed phase which can be determined independently from the mass balance as discussed above.

$$D(q) = D_0 \frac{d \ln p}{d \ln q} = \frac{D_0}{1 - \frac{q}{q_s}} = \frac{D_0}{1 - \frac{q}{q_0}\lambda} \tag{10}$$

In the nonlinear L_0, D corresponds to the diffusivity at infinite dilution, D_0, and the Henry law constant, which in the case of the Langmuir isotherm is given by $K = bq_s$. This means that, once the linear analysis is used to obtain L_{app} and $\frac{D}{R^2}$ from the fully equilibrated and partial loading experiments, the limiting L parameter can be calculated from $L_0 = (1 - \lambda)L_{app}$ and only λ is needed to match the experimental curves. Figure 5 shows the comparison between the experimental data from Fig. 4 and their nonlinear prediction.

The nonlinear model clearly provides an improvement of the match of the full loading data in the entire range of concentrations while predicting well also the partial loading and this is achieved by varying only the nonlinearity parameter. The results give a value of 0.444, which is below 0.5 and is indicative of a mild nonlinearity effect at the conditions of the experiment (Brandani 1998).

One additional advantage of the formulation of the nonlinear model is that it provides an easy way to calculate the equilibrium isotherm from the ZLC kinetic data. From Eq. 9, c_0 is known experimentally, q_0 is calculated applying the mass balance to the desorption curve, therefore once λ is determined, the Langmuir isotherm parameters b and q_s can be calculated allowing to retrieve the full isotherm. From
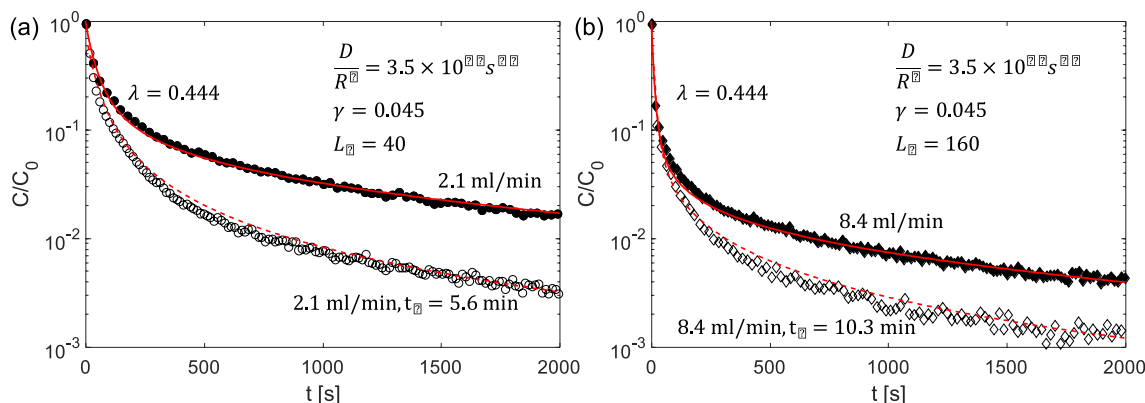

Fig. 5 Full and partial loading ZLC curves of 10% CO_2 in Na,Cs-Rho at **a** 2.1 ml/min and **b** 8.4 ml/min with ZLC nonlinear model predictions. Model parameters are reported in the plot
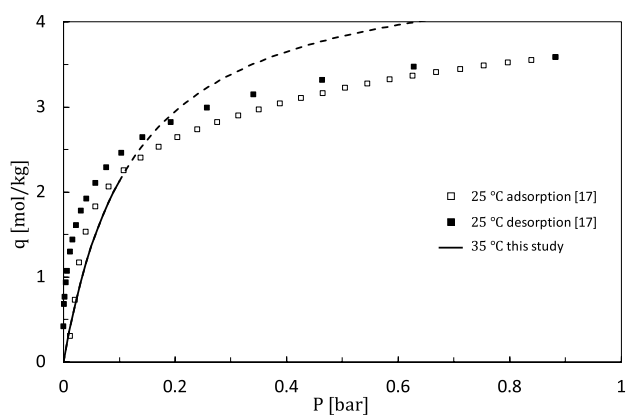
Fig. 6 Comparison between experimental CO_2 isotherm at 25 °C (Lozinska et al. 2012) and predicted at 35 °C from ZLC nonlinear analysis. Dotted line indicates the extrapolation of the predicted isotherm above 0.1 bar

the calculated CO_2 adsorbed amount ($q_0 = 2.13$ mol/kg) we obtain $q_s = 4.79$ mol/kg and this allows us to extract the CO_2 isotherm at 35 °C. Figure 6 shows the comparison between the calculated isotherm at 35 °C and the one measured at 25 °C using a Micromeritics ASAP 2020 volumetric system reported in our previous study (Lozinska et al. 2012). The ZLC data are only up to 0.1 bar and the dashed line is the extrapolation up to 1 bar. While the isotherm appears to cross the lower temperature data, the ZLC derived isotherm is closer to the true isotherm than the data from the volumetric system. Adsorption of CO_2 in a small pore zeolite should not result in a hysteresis, indicating that the volumetric measurements do not reach equilibrium and therefore the adsorption branch is actually below the true isotherm. This is consistent with the fact that the instrument used allows equilibration times for each adsorption/desorption point of up to 100 min, which is clearly below the saturation time required for this system. This indicates that conventional automated uptake measurements can be impractical with extremely slow adsorption processes. The ZLC provides an option for such systems with reasonable accuracy given that only one parameter is used to include the nonlinear effect. The fact that an accurate match of the kinetic curves can also be used to obtain type I isotherms has been demonstrated for CO_2 on 13X (Friedrich et al. 2015).

As a final example of what can be extracted from the experimental ZLC curves, the method proposed by Cavalcante (Cavalcante et al. 1995) is used to assess the diffusional path. The application of the analysis requires simply the plot of the desorption curve as c/c_0 vs $\sqrt{\frac{1}{t}}$ and the match with Eq. 6 (or 7 for slabs). The approach is valid for $\frac{c}{c_0} < 0.2$ and values of $L > 10$ but not too large in order to have a meaningful signal. The theory suggests to use $\frac{c}{c_0}L$ vs $\sqrt{\frac{1}{t}}$ if

multiple flowrates are available. Figure 7 shows the curves at 2.1 and 8.4 ml/min along with the theoretical line corresponding to a 3-D geometry. The experimental data are not perfectly overlapping because of the nonlinear effects but the intermediate analysis suggests an intercept close to -1, confirming that the system is characterised by a 3-dimensional isotropic diffusion path.

Conclusions

Technological advances in the field of gas diffusion measurements in nanoporous materials have often focussed on overcoming the difficulties to measure fast systems, and for this reason the challenges of measuring very slow system may be overlooked. Processes with slow kinetics pose a number challenges from the point of view of the instrumentation (signal/apparatus stability over long recording time), the experimental practicalities (long equilibration times) and the interpretation of the results. In this contribution we used the measurement of CO_2 in Na,Cs-Rho crystals as a case study to demonstrate how the ZLC system can be used as a powerful tool for the reliable assessment of the time constant of slow diffusion processes. For these systems, kinetic measurements cannot rely only on the use of the classic full loading experiment at different flowrates as this may lead to an incorrect interpretation of the time constant. Coupling the full loading to the partial loading experiment is therefore essential to extract the correct time constant of the process. The kinetic response of CO_2 in Na,Cs-Rho showed also evidence of a mild nonlinearity which was taken into account using the nonlinear solution of the ZLC model. This not only
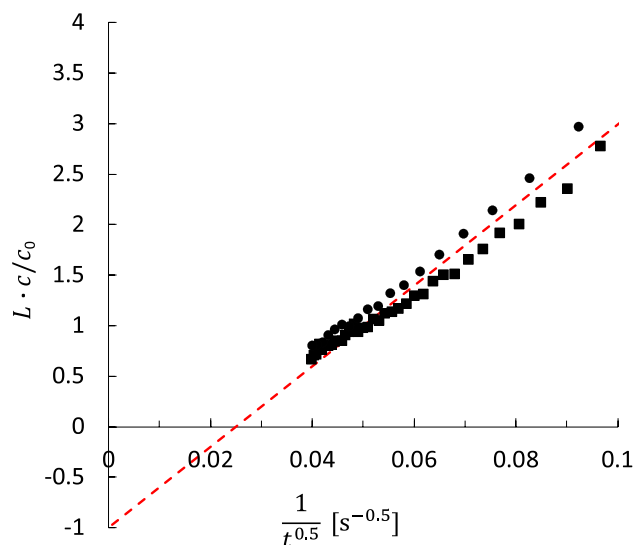

Fig. 7 ZLC intermediate time analysis for the full loading experiments at 2.1 and 8.4 ml/min. In red the model prediction, Eq. 6

improved the model prediction, but it also allowed to generate the CO_2 equilibrium isotherm on Na,Cs-Rho. Finally, the use of the intermediate time analysis confirmed that the diffusional path of the system aligns with the spherical diffusion model.

Prof. Cavalcante was the first to use the ZLC technique to measure adsorption processes with diffusional time constant of several hours, which are, to date, the slowest ever measured in a ZLC setup. His early work on the use of the ZLC system revealed to be highly valuable and inspirational to the design of our approach and the interpretation of the results. This contribution is meant to celebrate his many achievements in the field of adsorption engineering, looking forward to the many more to come.

Declarations

Conflict of interest On behalf of all authors, the corresponding author states that there is no conflict of interest.

References

Baerlocher C, McCusker LB, Olson DH (2007) Atlas of zeolite framework types. Elsevier Science

Barthelet K, Marrot J, Riou D, Férey G (2002) A breathing hybrid organic-inorganic solid with very large pores and high magnetic characteristics. Angew Chemie Int Ed 41:281–284. https://doi.org/10.1002/1521-3773(20020118)41:2%3c281::AID-ANIE281%3e3.0.CO;2-Y

Brandani S (1998) Effects of nonlinear equilibrium on zero length column experiments. Chem Eng Sci 53:2791–2798. https://doi.org/10.1016/S0009-2509(98)00075-X

Brandani S (2016) A simple graphical check of consistency for zero length column desorption curves. Chem Eng Technol 39:1194–1198. https://doi.org/10.1002/ceat.201500634

Brandani S, Mangano E (2021) The zero length column technique to measure adsorption equilibrium and kinetics: lessons learnt from 30 years of experience. Adsorption 27:319–351. https://doi.org/10.1007/s10450-020-00273-w

Brandani S, Ruthven DM (1995) Analysis of ZLC desorption curves for liquid systems. Chem Eng Sci 50:2055–2059. https://doi.org/10.1016/0009-2509(95)00048-A

Brandani S, Ruthven DM (1996) Analysis of ZLC desorption curves for gaseous systems. Adsorption 2:133–143. https://doi.org/10.1007/BF00127043

Brandani S, Hufton J, Ruthven D (1995) Self-diffusion of propane and propylene in 5A and 13X zeolite crystals studied by the tracer ZLC method. Zeolites 15:624–631. https://doi.org/10.1016/0144-2449(95)00042-5

Cavalcante CLJ, Ruthven DM (1995) Adsorption of branched and cyclic paraffins in silicalite. 2. Kinetics. Ind Eng Chem Res 34:185–191. https://doi.org/10.1021/ie00040a018

Cavalcante CL, Eić M, Ruthven DM, Occelli ML (1995) Diffusion of *n*-paraffins in offretite-erionite type zeolites. Zeolites 15:293–307. https://doi.org/10.1016/0144-2449(94)00061-V

Cavalcante CL, Brandani S, Ruthven DM (1997) Evaluation of the main diffusion path in zeolites from ZLC desorption curves. Zeolites 18:282–285. https://doi.org/10.1016/S0144-2449(97)00014-6

Eic M, Ruthven DM (1988) A new experimental technique for measurement of intracrystalline diffusivity. Zeolites 8:40–45. https://doi.org/10.1016/S0144-2449(88)80028-9

Friedrich D, Mangano E, Brandani S (2015) Automatic estimation of kinetic and isotherm parameters from ZLC experiments. Chem Eng Sci 126:616–624. https://doi.org/10.1016/j.ces.2014.12.062

Georgieva VM, Bruce EL, Verbraeken MC, Scott AR, Casteel WJ, Brandani S et al (2019) Triggered gate opening and breathing effects during selective CO_2 adsorption by merlinoite zeolite. J Am Chem Soc 141:12744–12759. https://doi.org/10.1021/jacs.9b05539

Gorring RL (1973) Diffusion of normal paraffins in zeolite T. Occur Window Effect J Catal 31:13–26. https://doi.org/10.1016/0021-9517(73)90265-0

Greenaway AG, Shin J, Cox PA, Shiko E, Thompson SP, Brandani S et al (2015) Structural changes of synthetic paulingite (Na, H-ECR-18) upon dehydration and CO_2 adsorption. Z Krist Cryst Mater 230:223–231. https://doi.org/10.1515/zkri-2014-1824

Hu X, Brandani S, Benin AI, Willis RR (2015a) Development of a semiautomated zero length column technique for carbon capture applications: rapid capacity ranking of novel adsorbents. Ind Eng Chem Res 54:6772–6780. https://doi.org/10.1021/acs.iecr.5b00513

Hu X, Brandani S, Benin AI, Willis RR (2015b) Development of a semiautomated zero length column technique for carbon capture applications: study of diffusion behavior of CO_2 in MOFs. Ind Eng Chem Res 54:5777–5783. https://doi.org/10.1021/acs.iecr.5b00515

Hufton JR, Ruthven DM (1993) Diffusion of light alkanes in silicalite studied by the zero length column method. Ind Eng Chem Res 32:2379–2386. https://doi.org/10.1021/ie00022a022

Lee Y, Reisner BA, Hanson JC, Jones GA, Parise JB, Corbin DR et al (2001) New insight into cation relocations within the pores of zeolite rho: in situ synchrotron X-ray and neutron powder diffraction studies of Pb- and Cd-exchanged rho. J Phys Chem B 105:7188–7199. https://doi.org/10.1021/jp0100349

Li (Kevin) G, Shang J, Gu Q, Awati RV, Jensen N, Grant A et al (2017) Temperature-regulated guest admission and release in microporous materials. Nat Commun 8:15777. https://doi.org/10.1038/ncomms15777

Lozinska MM, Mangano E, Mowat JPS, Shepherd AM, Howe RF, Thompson SP et al (2012) Understanding carbon dioxide adsorption on univalent cation forms of the flexible zeolite Rho at

conditions relevant to carbon capture from flue gases. J Am Chem Soc 134:17628–17642. https://doi.org/10.1021/ja3070864

Lozinska MM, Mowat JPS, Wright PA, Thompson SP, Jorda JL, Palomino M et al (2014) Cation gating and relocation during the highly selective "trapdoor" adsorption of CO_2 on univalent cation forms of zeolite rho. Chem Mater 26:2052–2061. https://doi.org/10.1021/cm404028f

Magalhães FD, Laurence RL, Conner WC (1996) Transport ofn-paraffins in zeolite T. AIChE J 42:68–86. https://doi.org/10.1002/aic.690420108

Palomino M, Corma A, Jordá JL, Rey F, Valencia S (2012) Zeolite Rho: a highly selective adsorbent for CO_2/CH_4 separation induced by a structural phase modification. Chem Commun 48:215–217. https://doi.org/10.1039/C1CC16320E

Remy T, Baron GV, Denayer JFM (2011) Modeling the effect of structural changes during dynamic separation processes on MOFs. Langmuir 27:13064–13071. https://doi.org/10.1021/la203374a

Serre C, Millange F, Thouvenot C, Noguès M, Marsolier G, Louër D et al (2002) Very large breathing effect in the first nanoporous chromium(III)-based solids: MIL-53 or Cr III (OH)·{O_2 C−C_6 H_4−CO_2}·{HO_2 C−C_6 H_4−CO_2H}$_x$ ·H_2Oy. J Am Chem Soc 124:13519–13526. https://doi.org/10.1021/ja0276974

Shang J, Li G, Singh R, Gu Q, Nairn KM, Bastow TJ et al (2012) Discriminative separation of gases by a "molecular trapdoor" mechanism in chabazite zeolites. J Am Chem Soc 134:19246–19253. https://doi.org/10.1021/ja309274y

Shang J, Li G, Singh R, Xiao P, Liu JZ, Webley PA (2013) Determination of composition range for "molecular trapdoor" effect in chabazite zeolite. J Phys Chem C 117:12841–12847. https://doi.org/10.1021/jp4015146

Zhao Y-P, Li Y, Cui C-Y, Xiao Y, Li R, Wang S-H et al (2016) Tetrazole–viologen-based flexible microporous metal-organic framework with high CO_2 selective uptake. Inorg Chem 55:7335–7340. https://doi.org/10.1021/acs.inorgchem.6b00320